View metadata, citation and similar papers at core.ac.uk
brought to you by CORE
provided by Elsevier - Publisher Connector

Available online at www.sciencedirect.com
ScienceDirect
Procedia Materials Science 3 (2014) 129 – 134
Procedia Materials Science
www.elsevier.com/locate/procedia

20th European Conference on Fracture (ECF20)

A finite fracture approach for determining the fracture onset of a brazed SiC specimen

E. Martin[a]*,T. Vandellos[b], D. Leguillon[c], E. Jacques[a], C. Lorrette[a]

[a]LCTS, CNRS UMR 5801, Université de Bordeaux, 3 rue La Boétie, F-33600 PESSAC, France
[b]ONERA-The French Aerospace Lab, F-92322 Châtillon, France
[c]IJLRA, CNRS UMR 7190, Université Pierre et Marie Curie, 4 place Jussieu, F-75252 PARIS Cedex 05, France

Abstract

The failure initiation of a brazed sample made of silicon carbide substrates and submitted to bending is analyzed with the help of a criterion which combines a maximum incremental energy release rate and a maximum tensile stress conditions. Two different modes of cracking are considered to develop in the vicinity of the free edge between the brazed layer and the ceramic substrate: edge debonding and substrate cracking. The comparison of the predictions with the experimental results allows estimating the fracture properties of the bonding.
© 2014 Published by Elsevier Ltd. Open access under CC BY-NC-ND license.
Selection and peer-review under responsibility of the Norwegian University of Science and Technology (NTNU), Department of Structural Engineering

Keywords: Brittle fracture; crack initiation; ceramics; brazing

1. Introduction

The prediction of the strength of a bonded joint classically relies on the analysis of the stress distribution near the bonded edge (Quispe Rodriguez et al., 2012) or in the use of linear elastic fracture mechanics (Chen et al., 2011). In each case a characteristic length is needed which must be determined experimentally. The recently introduced

* Corresponding author. Tel.: +33 5 56 84 47 00; fax: +33 5 56 84 12 25.
E-mail address: martin@lcst.u-bordeaux1.fr

2211-8128 © 2014 Published by Elsevier Ltd. Open access under CC BY-NC-ND license.
Selection and peer-review under responsibility of the Norwegian University of Science and Technology (NTNU), Department of Structural Engineering
doi:10.1016/j.mspro.2014.06.024

coupled strength and energy criterion (Leguillon, 2002) has proved to be successful to analyze the onset of fracture mechanisms within composite materials (Martin et al., 2010) (Martin et al., 2012) and bonded specimens (Nguyen et al., 2012) (Moradi et al., 2013a). This finite fracture mechanics approach relies on the assumption of a finite crack extension at fracture initiation. Coupling a stress condition with an energy analysis allows estimating the applied load and the nucleation length at crack onset without invoking a pre-existing flaw or using a characteristic distance.

The aim of this paper is to use the coupled criterion to predict the failure of a bonded specimen submitted to bending. The failure is assumed to initiate at the edges due to the presence of a stress singularity. This study is motivated by experimental results obtained with silicon carbide substrates bonded with a brazed layer (Jacques, 2012) and which demonstrate two modes of failure: i) interfacial propagation at the substrate/bond layer, ii) substrate failure near the bonded edge. In both cases, the mechanical response is brittle and only gives access to the onset of fracture. The onsets of these two mechanisms are analyzed with the help of the coupled criterion and it will be shown that the comparison with the experimental results allows estimating the interfacial fracture properties of the bonding.

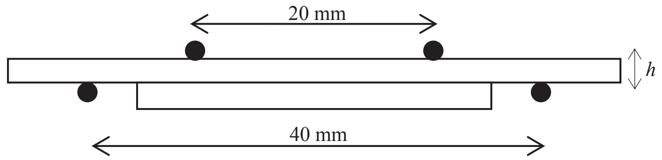

Fig. 1. The geometry of the specimen tested under four-point bending.

2. The coupled criterion

As proposed by Leguillon (2002), combining an energy and a stress condition allows to derive an initiation criterion in the vicinity of a stress concentration. First, an energy balance between an elastic state prior to any crack growth and after the onset of a crack extension of area δS leads to

$$\delta W + \delta W^k + G^c \delta S = 0 , \quad (1)$$

where δW is the change in potential energy, δW^k the change in kinetic energy and $G^c \delta S$ the fracture energy (G^c is the material toughness). Under the assumption of plane elasticity, the increment area is $\delta S = at$ is where a is the crack length and t the specimen thickness. This energy balance leads to an incremental energy condition with

$$\delta W^k \geq 0 \Rightarrow -\frac{\delta W}{\delta S} = G_{inc}\left(a\right) = A\left(a\right) E h \varepsilon^2 \geq G^c , \quad (2)$$

where ε is the remote applied strain, E is the material modulus, h is a structural length, and G_{inc} is the incremental energy release rate in which the infinitesimal energy rates of the classical Griffith approach are replaced by finite energy increments. If the scaling coefficient $A(a)$ is an increasing function of the crack length (which can be checked in many cases of stress concentration), the relation (2) provides a lower bound of the crack increment for a given value of the applied loading.

Second, a stress condition states that the opening normal stress σ_{op} along the anticipated path of crack nucleation is greater than the relevant strength σ^c

$$\sigma_{op}\left(x\right) = k_{op}\left(x\right) E \varepsilon \geq \sigma^c \text{ for } x \leq a . \quad (3)$$

If $k_{op}\left(x\right)$ is a decreasing function of the crack length (once again this can be checked in many cases of stress concentration), relation (3) provides an upper bound of the crack increment for a given value of the applied loading. Increasing the loading reduces the lower bound but increases the upper bound. Finally, for a monotonic and increasing applied loading, the crack increment at nucleation a^* is obtained by combining the equalities in (2) and (3) which leads to

$$\frac{A(a^*)}{k_{op}(a^*)} = \frac{1}{h}\frac{EG^c}{(\sigma^c)^2} . \quad (4)$$

The left hand side member of (4) is an increasing function of a^* vanishing for $a^* = 0$ so that this equation has always a solution and shows that the initiation length is not a material property but depends both on the characteristic fracture length $L^c = EG^c / (\sigma^c)^2$ and on the geometry of the structure. Once the initiation length a^* is determined, the initiation strain ε^* equivalently derives either from the energy condition or from the stress condition with

$$\varepsilon^* = \frac{\sigma^c}{Ek_{op}(a^*)} = \sqrt{\frac{G^c}{A(a^*)Eh}} . \quad (5)$$

Using the asymptotic expansion of the displacement field of the elastic solution, this approach was shown to provide a closed form expression which reveals accurate to predict the crack onset initiation at a sharp notch (Leguillon and Yosibash, 2003). It is here applied to analyse the initiation of fracture mechanisms near the free edge between the bond and the substrate.

3. Results and discussion

The geometry of the specimen tested under four-point flexure is schematized in Fig. 1. It consists of two substrates with the same thickness *h*= 2 mm bonded with a thin interlayer (thickness *e*= 0.3 mm). The elastic properties of the substrate (Hexoloy ®, St Gobain Advanced Ceramics) are selected to be $E_s = 430$ GPa (Young's modulus) and $\nu_s = 0.14$ (Poisson's ratio). The elastic properties of the interlayer are related to the brazing process which produces a porous layer and it is assumed that the relevant modulus E_l is lower than E_s with $E_l = 0.1E_s$ and that the Poisson's ratio is $\nu_l = 0.2$. Experimental results (Jacques, 2012) have evidenced two different modes of failure which develop near the free edges between the bond and the upper substrate: edge debonding (Fig. 2a) and substrate cracking (Fig. 2b). Due to the symmetry of the loaded specimen, it is assumed that each mechanism develops near each free edge. The onsets of those two cracking mechanisms are now analyzed with the help of the coupled criterion. A bidimensional finite element procedure with strongly refined mesh is used to derive the results which are presented. The computations confirm that the tensile stress is the main driving stress for each mechanism.

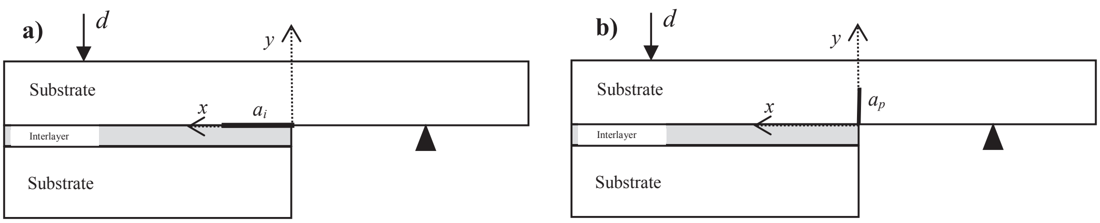

Fig. 2. Modes of failure: (a) edge debonding; (b) substrate craking; (only one half of the specimen is schematized).

3.1. Onset of edge debonding

For this interfacial crack path, the two conditions of the coupled criterion write

$$\begin{cases} \sigma_{yy}(x) = E_i\left(\dfrac{d}{h}\right)k_{yy}(x) \geq \sigma_i^c, \text{ for } x \leq a_i \\ G_{inc}(a_i) = E_i h\left(\dfrac{d}{h}\right)^2 A_i(a_i) \geq G_i^c \end{cases} \quad (6)$$

where a_i is the length of the debonding crack, d is the loading displacement, σ_i^c is the tensile interfacial strength ,

G_i^c is the interfacial toughness, $E_i = 2\left(\frac{1-\nu_l^2}{E_l} + \frac{1-\nu_s^2}{E_s}\right)^{-1}$ is an effective modulus. Fig. 3a plots the dimensionless coefficients (k_{yy}, A_i) versus the debonding length. This figure reveals that the incremental energy release rate always exhibits a maximum value for $a_i = a_i^{\max} \approx 0.1h$. The crack length a_i^* at debonding onset is thus bounded by $a_i^{\max}$ with $a_i^* \le a_i^{\max}$. Introducing the structural length $L_i^{\max} = \frac{A_i\left(a_i^{\max}\right)}{\left[k_{yy}\left(a_i^{\max}\right)\right]^2} h \approx 1.2h$, it can be shown that a sufficiently large value of the fracture length with $L_i^c = E_i \frac{G_i^c}{\left[\sigma_i^c\right]^2} \ge L_i^{\max}$ implies that the energy condition is the governing one (Martin et al., 2008). This condition is satisfied if $\sigma_i^c \le \sqrt{\frac{E_i G_i^c}{L_i^{\max}}}$. In this case, the applied displacement d_i^* at the initiation of edge debonding does not depend on the interfacial tensile strength and is given by

$$d_i^* = h\sqrt{\frac{G_i^c}{E_i h A_i\left(a_i^{\max}\right)}} \quad . \tag{7}$$

The predicted value of d_i^* is thus increasing with the interfacial toughness as plotted in Fig. 3b.

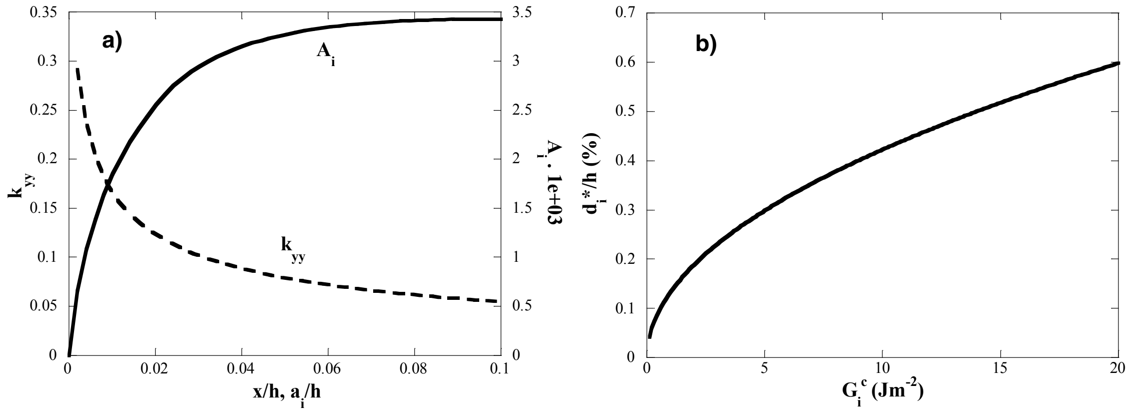

Fig. 3. Edge debonding: (a) Dimensionless coefficients vs. the normalized debonding length; (b) Applied displacement at debonding onset obtained with relation (7).

3.2. Onset of substrate penetration

Assuming now that substrate cracking occurs as depicted in Fig. 2b, the two conditions of the coupled criterion provides

$$\begin{cases} \sigma_{xx}(y) = E_s\left(\frac{d}{h}\right)k_{xx}(y) \ge \sigma_s^c \text{ , for } y \le a_p \\ G_{inc}\left(a_p\right) = E_s h\left(\frac{d}{h}\right)^2 A_p\left(a_p\right) \ge G_s^c \end{cases} \tag{8}$$

where a_p is the length of the crack, σ_s^c and G_s^c are respectively the tensile strength and the toughness of the substrate. Fig. 4a plots the dimensionless coefficients $\left(k_{xx}, A_p\right)$ versus the crack length. This figure indicates that the nucleation length a_p^* is bounded by $a_p^{\max} \approx 0.5h$ as a result of the compression state introduced in the upper substrate by the bending geometry. The applied displacement d_s^* at cracking onset now depends on the substrate tensile strength as shown by Fig. 4b.

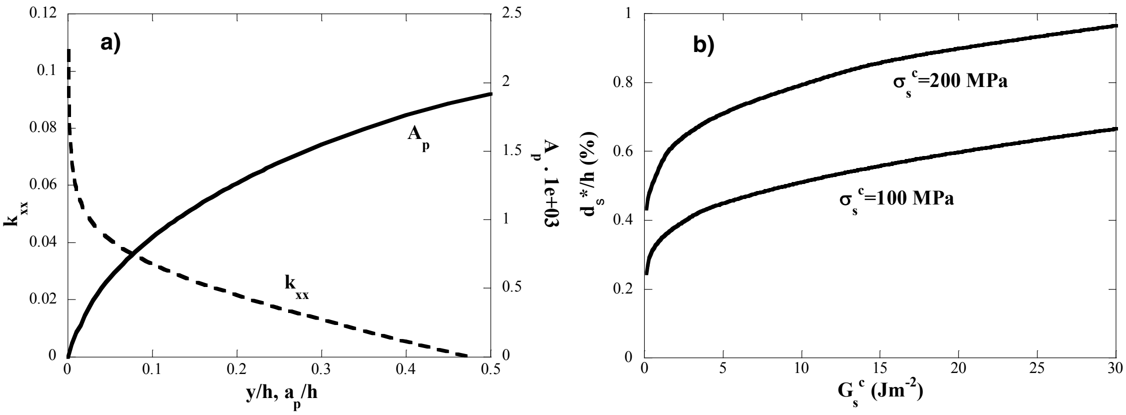

Fig. 4. Substrate cracking: (a) Dimensionless coefficients vs. the normalized cracking length; (b) Applied displacement at cracking onset.

3.3. Comparison with experimental results

Table 1 reports the measured displacement applied at onset of cracking modes for several brazed samples. Using the previous analysis, those values allow estimating the interfacial toughness of the brazed bond.
Edge debonding is assumed to result from a weak bonding (*i.e.* a low value of the interfacial tensile strength σ_i^c such that $\sigma_i^c \le \sqrt{\frac{E_i G_i^c}{L_i^{\max}}}$). In this case, the interfacial toughness can be directly derived from (7) with $G_i^c = E_i h\left(\frac{d_i^*}{h}\right)^2 A_i\left(a_i^{\max}\right)$ as indicated in Table 1.

Table 1. Experimental data (Jacques, 2013) and derived interfacial properties of the brazed bond.

Samples	Damage mode	d^*/h (%)	G_i^c (Jm^{-2})	σ_i^c (MPa)
1	Edge debonding	0.35	6.8	< 15.3
2	Edge debonding	0.25	3.5	< 11
3	Edge debonding	0.15	1.2	< 6.5
4	Substrate cracking	1	> 55.9	< 43.8
5	Substrate cracking	0.75	> 31.4	< 32.9
6	Substrate cracking	0.85	> 40.3	< 37.26

Substrate cracking implies that relation (8) is first satisfied prior to (6) if the competition with edge debonding is considered. It is thus assumed that the relation $G_i^c = E_i h \left(\frac{d_s^*}{h} \right)^2 A_i \left(a_i^{\max} \right)$ only provides a lower bound of the interfacial toughness as reported in Table 1.

Fracture properties of the SiC substrate have been characterized at room temperature leading to $\sigma_s^c =$ 234 MPa and $G_s^c \approx 30$ Jm^{-2} (Lorrette et al., 2013). Using those values to predict the cracking onset leads to $d_s^*/h = 1\%$ which is in good agreement with the experimental results. It is worthy of note that the characteristic fracture length of the substrate $L_s^c = E_s \frac{G_s^c}{\left(\sigma_s^c\right)^2} \approx 0.08h$ is small which implies that the initiation length is $a_s^* \approx 0.015h$ and will allow the use of an asymptotic approach to obtain simpler semi-analytical expression of the criterion (Moradi et al., 2013b).

4. Conclusion

A fracture criterion based on energy and stress conditions was used in order to analyze the crack onset of edge debonding and substrate cracking within a brazed specimen submitted to flexural loading. This finite fracture approach allows estimating the interfacial fracture energy in the case of weak bonding or its lower bound if substrate cracking is observed. It is a simple and powerful tool to estimate fracture properties when only crack onset data are available. More accurate results will require determining the influence of the modulus and the thickness of the brazed layer on the prediction of the applied displacement at crack onset.

References

Chen, Z., Adams, R.D., da Silva, L.F.M., 2011. Prediction of crack initiation and propagation of adhesive lap joints using an energy failure criterion. Engineering Fracture Mechanics. 78, 990–1007.

Jacques, E. PhD Thesis, University of Bordeaux, 2012.

Leguillon, D., 2002. Strength or toughness ? A criterion for crack onset at a notch. European Journal of Mechanics A/Solids 21, 61–72.

Leguillon, D., Yosibash, Z., 2003. Crack onset at a V-notch. Influence of the notch tip radius. International Journal of Fracture, 122, 1-21.

Lorrette, C., Réau, A., Briottet, L., 2013. Mechanical properties of nanostructured silicon carbide consolidated by spark plasma sintering. Journal of the European Ceramic Society. 33, 147–56.

Martin, E., Poitou, B., Leguillon, D., Gatt, J. M., 2008. Competition between deflection and penetration at an interface in the vicinity of a main crack. International Journal of Fracture, 151, 247–268.

Martin, E., Leguillon, D., Carrère, N., 2010. A twofold strength and toughness criterion for the onset of free-edge shear delamination in angle-ply laminates. International Journal of Solids and Structures. 47, 1297–305.

Martin, E., Leguillon, D., Carrère, N., 2012. A coupled strength and toughness criterion for the prediction of the open hole tensile strength of a composite plate. International Journal of Solids and Structures, 49, 3915–3922.

Moradi, A., Carrère, N., Leguillon, D., Martin, E., Cognard, J.Y., 2013a. Strength Prediction of Bonded Assemblies Using a Coupled Criterion under Elastic Assumptions: Effect of Material and Geometrical Parameters. International Journal of Adhesion and Adhesives 47: 73–82.

Moradi, A., Leguillon, D., Carrère, N., 2013b. Influence of the adhesive thickness on a debonding – An asymptotic model. Engineering Fracture Mechanics, 114, 55–68.

Nguyen, L.M., Leguillon, D., Gillia, O., Riviére, E., 21012. Bond failure of a SiC/SiC brazed assembly. Mechanics of Materials. 50:1–8.

Quispe Rodríguez, R. de Paiva, W.P., Sollero, P., Bertoni Rodrigues, M.R., de Albuquerque, ÉL, 2012. Failure criteria for adhesively bonded joints. International Journal of Adhesion and Adhesives, 37, 26–36.